First-Principles Study of Defect-Induced Magnetism in Carbon

Y. Zhang,[1,2] S. Talapatra,[3,*] S. Kar,[4] R. Vajtai,[2] S. K. Nayak,[1,2,†] and P. M. Ajayan[4,2]

[1]*Department of Physics, Applied Physics and Astronomy, Rensselaer Polytechnic Institute, Troy, New York 12180-3590, USA*
[2]*Rensselaer Nanotechnology Center, Rensselaer Polytechnic Institute, Troy, New York 12180-3590, USA*
[3]*Department of Physics, Southern Illinois University, Carbondale, Illinois 62901-4401, USA*
[4]*Department of MS & E, Rensselaer Polytechnic Institute, Troy, New York 12180-3590, USA*

(Received 30 December 2005; revised manuscript received 25 February 2007; published 7 September 2007)

We have studied the role of defects on the magnetic properties of carbon materials using first-principles density functional methods. We show that, while the total magnetization decreases both for diamond and graphite with increase in vacancy density, the magnetization decreases more rapidly for graphitic structures. The presence of nitrogen nearby a vacancy is shown to produce larger macroscopic magnetic signals as compared to a standalone carbon vacancy. The results indicate the possibility of tuning magnetization in carbon by controlled defect generation and doping.

DOI: 10.1103/PhysRevLett.99.107201 PACS numbers: 75.75.+a, 72.80.Ng, 75.50.Pp

Recent experimental efforts that produced ferromagnetically interacting carbon systems [1–4] have renewed the interest in carbon magnetism. The prospect of producing nonmetallic magnets using pure carbon systems is promising because carbon magnets will have applications in diverse fields [5,6]. Indeed, experimental attempts have been already made for making magnetic materials in various carbon systems such as in graphite [1,2], carbon nanofoams [3] and nanodiamonds [4].

A number of theoretical studies have also been performed in order to provide an atomic level understanding of observed magnetism in carbon systems [7–18]. These investigations focused on the role of topological defects, surface curvature, presence of adatoms, and mixed hybridization in inducing magnetism in carbon systems. For example, first-principle density functional calculations of stacked graphitic fragments showed stable ferromagnetically ordered ground states due to zigzag edge states [14]. Similarly, magnetic properties of adatoms on graphite surfaces was studied in detail [15]. Hydrogen induced magnetism in single walled nanotubes, featuring induced spin polarization localized at the carbon adatom on the surface of the SWNT, was demonstrated recently [18].

One of the novel ways of manipulating magnetism in carbon structures is through vacancies. For example, spin-polarized density functional theory (DFT) calculations of the magnetic properties of the vacancies and vacancy-hydrogen complexes in hydrogen implanted graphite [17] show that these defects lead to a macroscopic magnetic signal as also seen in experiments [1]. Most of the theoretical studies performed on vacancy mediated carbon magnetism deals with sp^2 carbon. It is of fundamental importance to investigate defect-induced magnetism in carbon systems having a bonding configuration other than sp^2 hybridization. In this Letter, to understand how the presence of vacancies affects the induced magnetism in carbon and whether the effect is universal to different carbon allotropes, we have carried out extensive spin-polarized DFT calculations both in diamond and graphite structures. Our results indicate that relative spatial distribution among the vacancies plays a crucial role and is a determinant factor regarding the observed magnetic behavior in various carbon systems. We found that with increasing vacancy accumulation the magnetization decreases nonmonotonically. We also show that the presence of foreign species (for example nitrogen) near a carbon vacancy greatly influences the induced magnetization in graphite.

The calculations are performed using the Vienna *Ab Initio* Simulation Package (VASP) electronic structure code [19–22] based on plane-wave basis sets. We have used spin-polarized DFT based on the generalized gradient approximation of Perdew and Wang (PW91) functional [23]. The core electrons are presented using the projector augmented wave (PAW) method [24]. The energy cutoff for structural optimization is taken to be 300 eV in order to achieve total energy convergence within several meV. The convergence for geometry optimization is taken to be 10^{-6} hartree/a.u..

For the supercell of diamond we used $a = b = c = 10.91$ Å. Simulation of bulk diamond using this supercell corresponds to 216 carbon atoms: larger super cells of dimensions corresponding to $a = b = c = 14.54$ Å are considered for selected cases and found to give similar results. A Monkhorst-Pack $4 \times 4 \times 4$ k-point grid is used to sample the Brillouin zone.

The supercell of the graphite has dimensions of $a = 29.47$ Å, $b = 25.52$ Å, $c = 3.35$ Å. Simulation of bulk graphite using this supercell consists of one slab with 288 carbon atoms. We have also considered two layers of graphite in our supercell method and find no noticeable effect of interlayer coupling on the electronic and magnetic properties of these systems. A Monkhorst-Pack $4 \times 4 \times 1$ k-point grid is used to sample the Brillouin zone.

First we consider the case of vacancy defects in diamond. The structure is relaxed after the vacancy is created. The nearest neighbor atoms of vacancy have a maximum displacement of 0.14 Å from the equilibrium position. The undercoordinated carbon atoms move closer to their immediate neighbors uniformly along the bonds. Our calculations show that one single vacancy in diamond leads to a ground state with a magnetic moment of $2\mu_B$. The nonmagnetic state is 0.24 eV higher than the ground state. The vacancy leaves four undercoordinated carbon atoms and each of them have dangling bonds which still have sp^3 hybridization. The four dangling orbitals give rise to four energy levels: three lie near the Fermi energy. The fourth one lies below the Fermi energy and is fully occupied with two of the electrons from the dangling bonds (see Fig. 1). The remaining three orbitals split with splitting energies of 0.9 eV between the polarized levels for spin-up and spin-down electrons. The remaining two electrons now occupy the spin-up energy levels giving rise to a net magnetic moment of $2\mu_B$.

However, introducing a second vacancy in the diamond cell influences the total magnetic moment. We have investigated various possible topological configurations for two vacancies within 5 Å. (The electronic and magnetic properties do not change with distances between the two vacancies larger than 5 Å). The topological configurations of the structure are shown in the Fig. 2 with corresponding magnetic moments listed in Table I. Since the spin-polarized levels are derived from the dangling bonds, the spin densities (not shown) are found to be localized on the undercoordinated atoms. In the X_a case with vacancy separation of 4.45 Å, all undercoordinated atoms are separated by at least one atom. The total magnetic moment is twice of that for the single vacancy. When the distance between the vacancies decreases, some of the undercoordinated atoms resulting from two different vacancies become nearest neighbors. This gives rise to a further increase in the bond order between the undercoordinated atoms (between single and double bonds) as found from the bond distance between them. As a result some of the previously unpaired electrons now contribute to bonding, resulting in a reduced magnetic moment in the system.

For example, in the configuration of two vacancies in the diamond supercell of X_0 and X_c (Fig. 2), two of the dangling atoms from vacancy X_0 become neighbors of two dangling atoms from vacancy X_c. The bond lengths between these dangling atoms are shortened to 1.41 Å. The total magnetic moment is reduced to $1\mu_B$ per vacancy in contrast to $2\mu_B$ observed both in the single vacancy case as well as when the distance between two vacancies is 4.45 Å or larger (Table I).

In order to obtain the energy difference between different magnetic states and the nonmagnetic state we have carried out fixed spin moment calculations. Interestingly, for all the distances we have studied, magnetic states are found to be the ground states (see Table I). The energy difference between the magnetic ground states and nonmagnetic states are noticeable, particularly when the distance between the vacancies is more than 4.0 Å. In addition, we have considered antiferromagnetic (AFM) coupling between the vacancies as a function of distance. We find that for the X_a position, the AFM state lies about 46 meV higher in energy compared to the ground state ferromagnetic state. For the X_b case, the energy difference between FM and AFM is found to be 26 meV, FM being the ground state. However, for X_c, AFM is found to be 7 meV lower in energy compared to the ferromagnetic state. The AFM states for other cases at short distances are found to be unstable and immediately converge to nonmagnetic states during self-consistent calculations. Although determining exact temperature at which the magnetic transition occurs requires detailed dynamic study [25], the above energetic results suggest that the vacancy-induced ferromagnetism in diamond structures (in particular at low vacancy concentration) should be observable in experiment at room temperature.

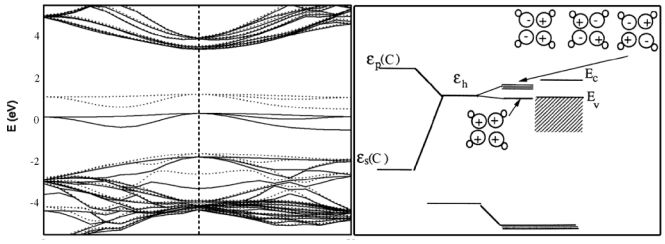

FIG. 1. Left: the electronic band structure of the diamond with a single vacancy per supercell. Bands for spin-up and spin-down electrons are represented by solid and dashed lines. Right: the dangling sp^3 hybrids coupled levels split to two groups.

Next we consider the effect of vacancy accumulation on magnetization in graphite. Previous DFT calculations have studied the energetics of various magnetic states as well as the nonmagnetic state for graphite with a single vacancy [15]. We find that the system with the single vacancy in graphite undergoes a Jahn-Teller distortion and breaks the graphene symmetry. Two of the dangling atoms move closer and form a weak bond. The displacements of dangling atoms lie between 0.14–0.17 Å. The ground state corresponds to a magnetic state which is in good agreement

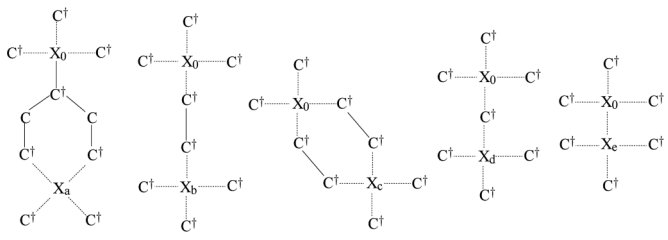

FIG. 2. Topological configuration of two vacancies in the diamond supercell. X_0 indicates the position of first vacancy, X_{a-e} indicates the relative position of the second vacancy. C† indicates undercoordinated carbon atoms, C indicates fourfold-coordinated carbon atoms.

TABLE I. Magnetic moment, distance between vacancies, and relative energy to ground state for different spin states for diamond.

2nd vacancy	Magnetic moment (μ_B)	Vacancy distance (Å)	$\Delta E(S=0)$	$\Delta E(S=2)$	ΔE(eV)$(S=4)$
X_a	4.00	4.45	0.50	0.36	0.00
X_b	2.00	3.96	0.12	0.00	0.79
X_c	2.022	3.01	0.02	0.00	0.51
X_d	2.00	2.57	0.10	0.00	0.15
X_e	2.00	1.57	0.06	0.00	1.25

with previous investigations [18]. We have also studied various topological configurations in the graphite systems as a function of distance between the vacancies. We find that the two vacancies behave like independent single vacancy—in terms of magnetic moment per vacancy—when the distance between them is 7 Å or larger. This should be compared to that of the diamond case where we find the minimum distance when the two vacancies exhibit atomic like moments is about 4.5 Å. All configurations for two vacancies for graphite case with distance of less than 7 Å considered are shown in Fig. 3. Table II shows the energy difference between the magnetic and nonmagnetic states as a function of distance between the two vacancies. The variation of magnetic moment is nonmonotonic as a function of distance. More importantly the energy difference between the magnetic and nonmagnetic states is smaller compared to that in the diamond structures. Comparing to the sp^3 hybridization in diamond, the bonds in the graphite sp^2 hybridization has more flexibility to change the bond order. The local bonding environment around the vacancy relaxes its structure and forms bonds that are stronger than typical sp^2 C-C bonds. Some of the dangling electrons introduced by vacancy are accommodated in the newly strengthened bonds and therefore are not available for localized spin-polarized levels. We also carried out total energy calculations for AFM states in graphite systems. The AFM states for X_b is about 23 meV higher in energy compared to the FM ground state, while for X_g AFM is found to be 4 meV higher in energy (degenerate) compared to the FM state. These results suggest that it may be easier to observe vacancy-induced magnetism in diamonds particularly at room temperature compared to that in graphite. This could have impact in making nonmetal based magnetic structures.

The importance of the bonding environment in observing carbon magnetism was experimentally demonstrated by ion irradiation of graphite and diamond [1,4]. The effect of nitrogen impurities on the magnetism of the graphitic system was also studied extensively using DFT methods. By considering the most favorable configurations for nitrogen impurities, it was shown that nitrogen adsorbed on the surface of graphite or carbon nanotube possesses finite magnetic moments [26]. To verify the effect of the bonding environment nearby a vacancy we considered a possible

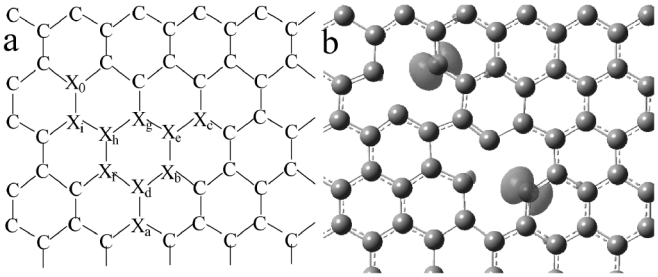

FIG. 3. (a) Topological configuration of two vacancies in the graphite supercell. X_0 indicates the position of first vacancy, X_{a-i} indicates the relative position of the second vacancy. (While for the cases of nitrogen implantation, X_0 indicates the position of vacancy, X_{a-i} indicates the relative position of the nitrogen atom.) (b) Spin density shown for the 2nd vacancy in the X_b position.

scenario where a N atom is present at different locations near a vacancy defect in graphite. N incorporation does not change the overall sp^2 bonding character in graphite structure and easily fits into the graphite network. However, our calculations show that the presence and position of a single N atom near a carbon vacancy in graphite has profound effects on the spin configurations of these systems. We found that the ground state of graphite with one substitutional nitrogen is nonmagnetic, in agreement with previous calculations [26], however, the total magnetic moment varies with the presence of N, as well as its relative distance from the vacancy. The results of our calculations are shown in Table III. The relative position of N and the vacancy is indicated in Fig. 3(a). Here the X_0 indicates the position of the vacancy while the X_{a-i} indicates the position of nitrogen.

For example, in the case of X_f in Fig. 3(a), the N atom is at a distance of 3.75 Å from the vacancy. The nitrogen atom is incorporated into the sp^2 network. The extra electron from nitrogen dissipates around the vacancy site and induces a small extra spin density on each of the undercoordinated carbon atoms. This results in an increase of the magnetic moment of the system as compared to a single

TABLE II. Magnetic moment, distance between vacancies, and relative energy to ground state for different spin states for graphite.

2nd vacancy	Magnetic moment (μ_B)	Vacancy distance (Å)	$\Delta E(S=0)$	$\Delta E(S=2)$	ΔE(eV)$(S=4)$
X_a	0.00	6.18	0.00	0.10	0.18
X_b	2.00	5.11	0.25	0.00	0.11
X_c	2.00	5.11	0.25	0.00	0.11
X_d	0.00	4.91	0.00	0.13	0.35
X_e	0.00	4.25	0.00	0.01	0.05
X_f	0.00	3.75	0.00	0.14	0.60
X_g	2.00	2.84	0.05	0.00	0.24
X_h	0.00	2.46	0.00	0.11	0.53
X_i	0.00	1.42	0.00	0.09	0.51

TABLE III. Magnetic moment and nitrogen-vacancy distance for the graphite. The vacancy position is indicated as X_0 in Fig. 3(a).

Nitrogen adatom position	Magnetic moment (μ_B)	Vacancy-Nitrogen distance (Å)
X_a	3.00	6.18
X_b	1.00	5.11
X_c	1.00	5.11
X_d	3.00	4.91
X_e	3.00	4.25
X_f	3.00	3.75
X_g	1.00	2.84
X_h	3.00	2.46
X_i	1.00	1.42

vacancy and suggests that a combination of vacancy defects and impurities may provide a unique way for enhancing the magnetic moment in graphite systems. Interestingly, the AFM state in the X_a case is found to be 32 meV higher in energy compared to the ferromagnetic state; which suggests that nitrogen doping further stabilizes the FM state compared to the pure graphite case.

In conclusion, we have shown that the presence of vacancies in carbon systems dominates the magnetic property. The total magnetization in graphite and diamond generally decreases with the decrease of the separation distance between the vacancy defects. In the case of diamond, the magnetism persists for larger vacancy concentrations while magnetism is observed in graphite for relatively low vacancy concentration. Also interstitial carbon atoms resulted from creation of vacancy possibly induce further magnetism with relative high Curie temperature [15]. The presence of a N impurity atom near a carbon vacancy, in the case of graphite, affects the local spin configuration near a vacancy as well as the energetic difference between the AFM and FM states. These results provide conclusive evidence that the magnetism in carbon structures due to vacancies depends strongly on their concentration as well as the local bonding environment. Though the physical phenomena governing the defect-induced magnetism in carbon structures is complicated, these calculations provides an insight into the probable mechanisms associated with this phenomenon and could lead to a better understanding of magnetism in carbon systems.

The present work was supported by the Nanoscale Science and Engineering Initiative of the National Science Foundation (No. DMR-0117792). We thank Philip Shemella for helpful discussions.

*stalapatra@physics.siu.edu
†nayaks@rpi. edu

[1] P. Esquinazi, D. Spemann, R. Höhne, A. Setzer, K.-H. Han, and T. Butz, Phys. Rev. Lett. **91**, 227201 (2003).
[2] P. Esquinazi, A. Setzer, R. Höhne, C. Semmelhack, Y. Kopelevich, D. Spemann, T. Butz, B. Kohlstrunk, and M. L. Han, Phys. Rev. B **66**, 024429 (2002).
[3] A. V. Rode, E. G. Gamaly, A. G. Christy, J. G. Fitzgerald, S. T. Hyde, R. G. Elliman, B. Luther-Davies, A. I. Veinger, J. Androulakis, and J. Giapintzakis, Phys. Rev. B **70**, 054407 (2004).
[4] S. Talapatra, P. G. Ganesan, T. Kim, R. Vajtai, M. Huang, M. Shima, G. Ramanath, D. Srivastava, S. C. Deevi, and P. M. Ajayan, Phys. Rev. Lett. **91**, 097201 (2003).
[5] T. L. Makarova, *Studies of High-Temperature Superconductivity* (NOVA Science, New York, 2003), p. 107.
[6] T. L. Makarova, Semiconductors **38**, 615 (2004).
[7] D. Khveshchenko, Phys. Rev. Lett. **87**, 206401 (2001).
[8] D. Khveshchenko, Phys. Rev. Lett. **87**, 246802 (2001).
[9] A. N. Andriotis, M. Menon, R. Sheetz, and L. Chernozatonskii, Phys. Rev. Lett. **90**, 026801 (2003).
[10] A. N. Andriotis, R. Sheetz, and M. Menon, J. Phys. Condens. Matter **17**, L35 (2005).
[11] A. N. Andriotis and M. Menon, *Clusters and Nano-Assemblies, Physical and Biological Systems* (Word Scientific, Singapore, 2005), p. 199.
[12] N. Park, M. Yoon, S. Berber, J. Ihm, E. Osawa, and D. Tomanek, Phys. Rev. Lett. **91**, 237204 (2003).
[13] Y. H. Kim, J. Choi, K. J. Chang, and D. Tomanek, Phys. Rev. B **68**, 125420 (2003).
[14] H. Lee, N. Park, Y. Son, S. Han, and J. Yu, Chem. Phys. Lett. **398**, 207 (2004).
[15] P. O. Lehtinen, A. S. Foster, A. Ayuela, A. Krasheninnikov, K. Nordlund, and R. M. Nieminen, Phys. Rev. Lett. **91**, 017202 (2003).
[16] P. O. Lehtinen, A. S. Foster, A. Ayuela, T. Vehvilainen, and R. M. Nieminen, Phys. Rev. B **69**, 155422 (2004).
[17] Y. Ma, P. O. Lehtinen, A. S. Foster, and R. M. Nieminen, Phys. Rev. B **72**, 085451 (2005).
[18] P. O. Lehtinen, A. S. Foster, Y. Ma, A. V. Krasheninnikov, and R. M. Nieminen, Phys. Rev. Lett. **93**, 187202 (2004).
[19] G. Kresse and J. Hafner, Phys. Rev. B **48**, 13 115 (1993).
[20] G. Kresse and J. Hafner, Phys. Rev. B. **49**, 14 251 (1994).
[21] G. Kresse and J. Furthmüller, Comput. Mater. Sci. **6**, 15 (1996).
[22] G. Kresse and J. Furthmüller, Phys. Rev. B. **54**, 11 169 (1996).
[23] J. P. Perdew, K. Burke, and Y. Wang, Phys. Rev. B. **54**, 16 533 (1996).
[24] P. E. Blochl, Phys. Rev. B. **50**, 17 953 (1994).
[25] M. Lezaić, P. Mavropoulos, and S. Blügel, Appl. Phys. Lett. **90**, 082504 (2007).
[26] Y. Ma, A. S. Foster, A. V. Krasheninnikov, and R. M. Nieminen, Phys. Rev. B. **72**, 205416 (2005).